Analytica Chimica Acta 759 (2013) 74–80

Contents lists available at SciVerse ScienceDirect

Analytica Chimica Acta

journal homepage: www.elsevier.com/locate/aca

Label-free electrochemical monitoring of vasopressin in aptamer-based microfluidic biosensors

Peng He[1], Vlad Oncescu, Seoho Lee, Inhee Choi, David Erickson*

Sibley School of Mechanical and Aerospace Engineering, Cornell University, Ithaca, NY 14853, United States

GRAPHICAL ABSTRACT

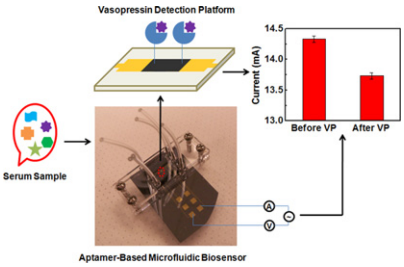

ARTICLE INFO

Article history:
Received 21 May 2012
Received in revised form 17 October 2012
Accepted 20 October 2012
Available online 12 November 2012

Keywords:
Biosensor
Aptamer
Vasopressin
Carbon nanotube

ABSTRACT

Vasopressin is an indicating biomarker for blood pressure in the human body and low vasopressin levels can be indicative of late-phase hemorrhagic shock or other traumatic injuries. In this paper we have developed an aptamer-based label-free microfluidic biosensor for the electrochemical detection of vasopressin. The detection area consists of aptamers immobilized on carbon nanotubes which specifically capture the vasopressin molecules in solution resulting in changes in conductivity across the sensor. We report a limit of detection of 43 pM in standard solutions and demonstrate high detection specificity toward vasopressin when different interferents are present. The miniaturized microfluidic biosensor offers continuous monitoring of different vasopressin levels with good potential for portability. Ultimately such a system could serve as a point-of-care diagnostics tool for patients with excessive bleeding when standard medical infrastructure is not available.

1. Introduction

Biomarkers are biological indicators whose levels vary when the physiological state of a biological system changes, often in response to a specific disease or infection state [1–6]. Such measurable biomarkers have been linked, among other things, to diabetes [7], cardiovascular disease [8], influenza [9], and various organ dysfunctions [10]. Therefore the development of diagnostic devices that can monitor biomarkers in a point-of-care setting is of paramount importance for disease diagnosis and treatment.

Recent advancements in lab-on-a-chip and microfluidic techniques have improved the accessibility of biomarker detection systems by requiring lower sample volumes, increasing the analysis speed and response time, allowing for massive parallelization for high-throughput analysis, and reducing the cost of fabrication of biosensors [11,12]. For example, electrochemical biosensors for evaluating blood glucose levels using the enzymatic oxidation of glucose in solution are well established and particularly important in fighting diabetes [13]. Lateral flow or immunochromatographic strip that tests for the detection of either antigens or antibodies of different viruses, such as human immunodeficiency virus (HIV) [14], hepatitis B virus (HBV) [15], and dengue virus [16], have been successfully implemented for use in the developing world over the past decade.

* Corresponding author at: 240 Upson Hall, Cornell University, Ithaca, NY 14853, United States. Tel.: +1 607 255 4861; fax: +1 607 255 1222.
E-mail address: de54@cornell.edu (D. Erickson).
[1] Present address: The Procter & Gamble Company, Product Safety & Regulatory Affairs, P&G Chemicals Research & Development, Cincinnati, OH 45241, United States.

0003-2670/$ – see front matter © 2012 Elsevier B.V. All rights reserved.
http://dx.doi.org/10.1016/j.aca.2012.10.038

In addition, recent developments in nanotechnology and related biotechnological applications have greatly promoted the miniaturization and integration of diagnostic devices with high sensitivity and specificity. For example, Stern et al. [17] has developed a label-free nanosensors in which a microfluidic purification chip simultaneously captures multiple biomarkers from blood samples and releases them into purified buffer for sensing using a silicon nanoribbon detector. Moreover, Wang et al. has demonstrated detection sensitivity at attomolar levels for protein tumor biomarkers in a variety of clinically relevant media with a linear dynamic range of over six orders of magnitude in a matrix-insensitive assay composed of a number of individually addressable magnet-nanosensors [18].

While this progress has been impressive, the application of these devices to diagnosing traumatic injuries has been limited [19]. Hemorrhagic shock for example is the number one cause of preventable death in military battlefield situations. Progression to late phase hemorrhagic shock due to prolonged hypotension is known to be indicated by a marked decrease of plasma vasopressin levels [20–22]. Vasopressin, a nine-amino acid peptide hormone, plays a key role in increasing peripheral vascular resistance, which in turn increases arterial blood pressure. Therefore, vasopressin can represent a suitable biomarker, indicative of cases where a patient who has experienced a significant traumatic injury has progressed to hemorrhagic shock. Most of vasopressin assay kits which are currently available on the market are either enzyme immunoassay (Arg-Vasopressin EIA kit; Assay Designs) or enzyme-linked immunosorbent assay (Arg-Vasopressin ELISA kit; Abnova) types. Quantification of vasopressin using such assays involves delicate sample preparation, sample extraction and reagent preparation that precede optical-based assay procedures in a laboratory setting. These methods are not easily adapted to emergency medicine situations or low resource environments. A simple and portable device that can rapidly monitor vasopressin could therefore enable more rapid determination of a patient's baseline health and survivability.

For that purpose, we have investigated promising recent developments in aptamer and carbon nanotube bio-sensing applications. Aptamers are short and stable single-stranded oligonucleic acid molecules that have been widely employed for specific binding to target molecules such as amino acids, drugs, and proteins [23–25]. Due to low nuclease degradation in the bloodstream, aptamers possess two significant advantages over other bioreceptors, namely high stability and specificity. A bioactive and nuclease-resistant aptamer specific for vasopressin, in the form of a fifty five-nucleotide single-stranded DNA spiegelmer, has already been reported in the literature [26–28]. The binding between aptamer and vasopressin can be transduced to a readable signal via different approaches in aptamer-based biosensors [29–32], however electrical transduction is often preferred due to the relative ease with which it can be measured and integrated with modern electronics [33–41].

Owing to their excellent electrical conductivity and chemical stability, carbon nanotubes (CNTs) show great potential in the development of advanced electrical biosensors [42,43]. The CNTs can be modified to function as carriers for electrical bioreceptors such as aptamers, offering an efficient platform to capture target molecules [44]. Since a single biomolecule present on or near the surface of a CNT, can alter the CNT's electronic properties through charge transfer, CNTs are very versatile for the design of new highly sensitive and selective biosensors for probing DNA, proteins and enzymes with different conductance properties. For example, CNTs were applied into aptamer-based biosensors to achieve 10 nM limit of detection of thrombin [45].

Toward the goal of developing a portable point-of-care diagnostic device for electrochemical monitoring of vasopressin, we present here an aptamer-based carbon nanotube biosensor integrated within a microfluidic system. The biosensor takes advantage of changes in conductivity caused by vasopressin binding on the aptamer-modified carbon nanotubes which are then converted to a changes in measureable current. The miniaturized device is also shown to continuously monitor changes in vasopressin concentration, which demonstrates the possibility of real-time detection of target molecules in a circulatory system. Finally, we demonstrate the electrochemical monitoring of vasopressin from standard solutions and sheep serum with a limit of detection (LOD) of 43 pM, on the same order of magnitude as the physiological level of vasopressin in the bloodstream which has been found to be approximately 6 ± 3 pM for healthy individuals and 52 ± 30 pM for patients with sepsis [46].

2. Materials and methods

2.1. Reagents and materials

Arginine vasopressin with Cys-Tyr-Phe-Gln-Asn-Cys-Pro-Arg-Gly-NH_2 sequence and lypressin with Cys-Tyr-Phe-Gln-Asn-Cys-Pro-Lys-Gly-NH_2 sequence were purchased from American Peptide Company Inc. Aptamer, 55-nt single-stranded DNA pool synthesized with the sequence 5′-TCACGTGCATGATAGACGGC GAAGCCGTCGAGTTGCTGTGTGCCGATGCACGTGA, was ordered from Integrated DNA Technologies Inc. COOH-functionalized multiwall carbon nanotubes were obtained from Cheap Tubes Inc. N-hydroxysuccinimide (NHS) and Sodium dodecylsulfate (SDS) were purchased from MP Biomedicals LLC, while 1-ethyl-3-(3-dimethylaminopropyl) carbodiimide (EDC) was purchased from Geno Technology, Inc Sheep Serum was obtained from Valley Biomedical Inc. and human serum albumin (HSA) was purchased from Sigma–Aldrich Co.

2.2. Apparatus

2.2.1. Patterning of CNTs and gold electrodes on silicon wafer

Fig. 1A shows the fabrication process for the microfluidic biosensor system. In this design CNTs were immobilized between two lithographically patterned gold electrodes with a gap of 10 μm. This gap was chosen for the CNT pattern because initial experiments have demonstrated increased sensitivity with decreasing gap in the 10–50 μm range. First a 4-in. silicon wafer was cleaned and oxidized in hot piranha solution in order to generate hydroxyl groups on its surface. Microposit S1805 Photo Resist was than spin-coated on the silicon wafer surface and the CNT pattern was created using standard photolithography. The silicon wafer was then treated in a Molecular Vapor Deposition Tool (MVD 100), undergoing a 15 min (3-aminopropyl)trimethoxysilane (APTMS) deposition in order to form an amine group monolayer on the wafer surface. Carbon nanotubes dispersed in 0.5% SDS solution (0.1 mg mL^{-1}) were pipetted on APTMS-treated CNT pattern and allowed to immobilize on the surface at room temperature for 3 h [47]. Subsequently, the wafer was oven-baked overnight at 80 °C.

The gold electrodes were patterned using a standard LOR3A lift-off process. The patterned CNTs were aligned with the gold electrode pattern and 5 nm chromium/60 nm gold were deposited on the wafer using an e-Beam Evaporator. Following the evaporation, the wafer was diced into 5 cm × 5 cm pieces (Fig. 1B).

2.2.2. Fabrication of patterned microchannels on polydimethylsiloxane (PDMS)

SU-8 2050 Permanent Epoxy Resist was spin-coated on a 4-in. silicon wafer. The resist-coated wafer was exposed to UV light under the shield of the microchannel pattern-designed photomask in an ABM Contact Aligner. The wafer was developed in SU-8 Developer for a few minutes. The mixture of 50 g PDMS and 5 g

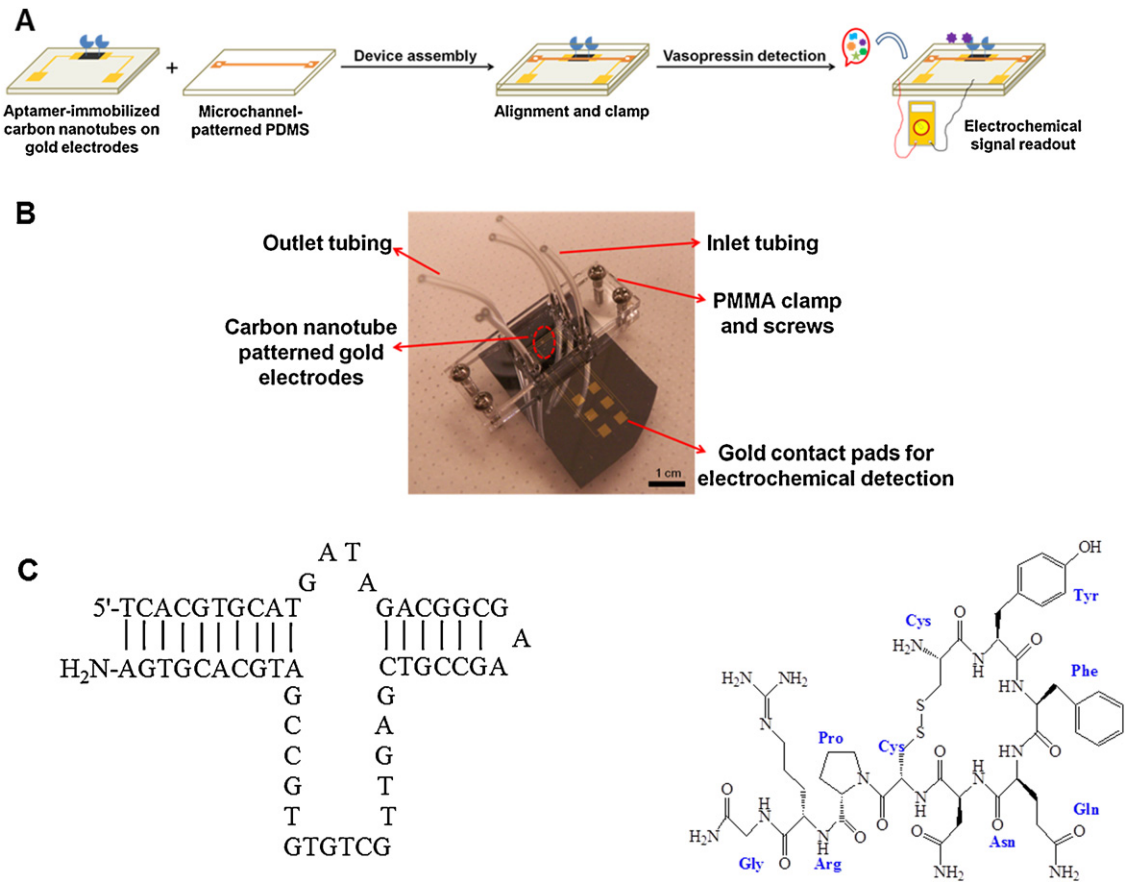

Fig. 1. (A) Schematic of fabrication process of aptamer-based microfluidic biosensor; (B) a photo picture of microfluidic device; and (C) chemical structures of aptamer (left) and vasopressin (right).

curing agent was filled in a Petri dish containing the wafer with the microchannel pattern and was degassed in vacuum for 15 min, followed by baking in oven at 80 °C for 3 h. The microchannel-patterned PDMS pieces were cut out after PDMS solidification.

2.2.3. Surface modification of patterned CNT on silicon wafer

The core of the sensing device is the signal-transducing carbon nanotubes with aptamer surface modification, which are amine-terminated fifty-five base oligonucleotides with a cyclic structure (Fig. 1C, left). It allows the tight binding of specific target, vasopressin molecules (Fig. 1C, right). Before the aptamer immobilization, a mixture of 0.4 M EDC and 0.1 M NHS in 1:1 volume ratio was pipetted on the CNT-immobilized pattern of the sensor. The mixture droplets were maintained on the pattern for 3 h at room temperature in order to create an EDC/NHS activation layer on which aptamers can effectively be immobilized [44]. Subsequently, the sensors were cleaned with DI H_2O wash and N_2 dry. Aptamer solution at 1 μM concentration was then pipetted on the EDC/NHS-modified CNTs and maintained for 24 h at room temperature for immobilization. The aptamer-modified sensors were once again cleaned with DI H_2O wash and N_2 dry. For both NHS/EDC and aptamer modifications, 1.5 μL of solution droplet was used per sensor to cover its detection area entirely. To prevent the premature drying of the droplets, the sensors were kept in a humidified chamber.

2.2.4. Device assembly

One silicon wafer piece (3 cm × 2 cm) contains three CNT-gold electrode pairs for multiple measurements in parallel. Holes were perforated in the microchannel-patterned PDMS piece on the inlet and outlet parts of microchannels. The CNT-gold electrodes on aptamer-conjugated silicon wafer were aligned with the microchannels by optical microscopy. PDMS-wafer integration setup was tightly sandwiched into two poly(methyl methacrylate) (PMMA) clamps with screws (Fig. 1B).

3. Results and discussion

3.1. SEM characterization of patterned CNTs

The technology behind nanoscale conducting materials such as semiconductor nanowires is well developed. However because of sophisticated laboratory fabrication processes and device-specific techniques for nanowire assembly, the development of nanowire sensors with desired electrical properties is still challenging. Incorporating a modified CNT surface between lithographically patterned electrodes is a simple and robust method of fabricating such sensors. Here, the patterned CNT area is 410 μm × 300 μm, which covers the gap between two gold electrodes (Fig. 2A). In this design, one biosensing chip contains three CNT-gold electrode pairs connected to the corresponding contact pads (Fig. 1B), which can take multiple sample measurements in parallel. The immobilized CNTs show excellent stability on the silicon wafer surface due to the amide bonding with APTMS when compared to physical adsorption. The outer diameter and length of CNTs are 8–15 nm and 10–50 μm respectively, offering the total surface area of 0.25–2.36 μm^2 for each CNT. The aptamer modification on the CNT surface was successfully confirmed by fluorescence microscopy after the incubation of fluorescent dye-labeled vasopressin on the aptamer-modified CNT surface. APTMS monolayer

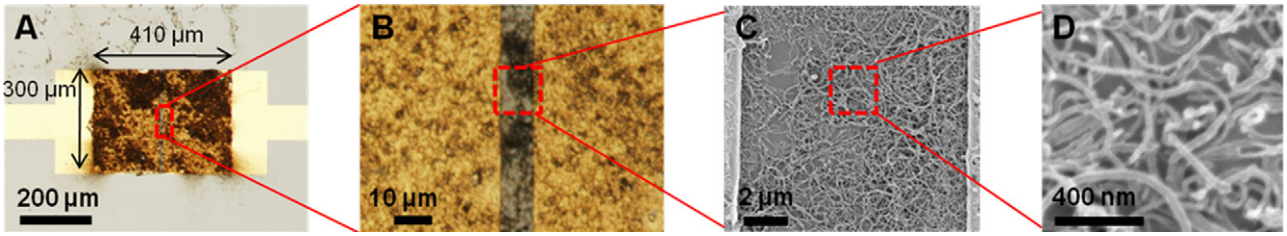

Fig. 2. (A) Optical image of carbon nanotube-patterned gold electrodes; (B) enlarged optical image of carbon nanotube distribution on the gold electrodes and gap; (C) scanning electron microscopic image of carbon nanotube distribution on the gap of gold electrodes; and (D) enlarged SEM image of carbon nanotube morphology.

deposition induced uniform distribution of CNTs, which allowed the flowing vasopressin-containing fluid to be fully in contact with aptamers on the surface allowing for maximum capture. The method developed here to assemble CNTs into the device structure is both rapid and robust with excellent reproducibility, which gives it an advantage over other more sophisticated methods such as chemical vapor deposition technique [45].

3.2. Sensitivity measurement of vasopressin detection in standard solutions

The current before and after vasopressin introduction into the detection system were measured and compared (Fig. 3A). The decrease ratio was calculated to be $4.18 \pm 0.61\%$ and it was found to be closely related to the captured amount of vasopressin in solution. Since there is some variation in conductivity along the patterned CNTs between different devices, the relative conductivity decrease ratio, instead of the absolute conductivity decrease, is a more appropriate indicator of detection performance for the biosensing device. Fig. 3B shows the calculated current decrease ratios in the microfluidic biosensor system at different concentrations of vasopressin in solution. The background noise is indicated by the decrease ratio of the negative control experiment ($0.23 \pm 0.02\%$) and can be employed to differentiate vasopressin solutions at concentrations lower than 100 pM. The negative control experiment was done using standard buffer solution without vasopressin. This achievable detection sensitivity in the current platform is similar to that of traditional vasopressin immunoassays and also comparable to the results of other biomarker detection on electrochemical nanosensors [48,49]. The volume of the microchannel overlapping the patterned CNTs for vasopressin detection is calculated to be 9 nL, given that the fabricated microchannel depth is 75 μm and the patterned CNT area is 0.12 mm^2 (Fig. 2). The result is equivalent to direct recognition of around 900 zeptomole of vasopressin in the label-free electrochemical detection. Detection of even smaller amount of vasopressin in solution is limited by the vasopressin–aptamer dissociation constant and Langmuir adsorption isotherm [27,50]. Limit-of-detection (LOD) for vasopressin in aptamer-based microfluidic biosensor is derived to be 43 pM from the linear relationship in the inset plot of Fig. 3B. The LOD in this case is the smallest vasopressin concentration that give a current decrease higher than the background noise. This LOD is of the same order as physiological concentration of vassopressin in humans. In a clinical study, Jochberger et al. revealed that although the plasma vasopressin concentration of healthy individuals is approximately 6 ± 3 pM, the concentration for patients with sepsis is 52 ± 30 pM [46]. The higher vasopressin concentration for patients for patients with sepsis is observed as their body attempts to reverse hypotension through the release of vasopressin. The late-phase HS which our biosensor aims to treat occurs when such attempts by the body fail, resulting in the drop of vasopressin concentrations from the unusually high levels. Therefore, plasma vasopressin concentration of interest is expected to be high initially (52 ± 30 pM), and the key for detecting the targeted disease is to detect a drop in vasopressin concentration from this initial value.

3.3. Specificity measurement of vasopressin detection in standard solutions

The developed biosensor's specificity for vasopressin was tested by examining its detection performance in complex serum containing two different interferents: HSA and lypressin. HSA is the most abundant protein in human body fluids and therefore specificity of our biosensor against HSA is crucial for our goal of monitoring plasma vasopressin without sample purification. On the other hand, lypressin has remarkably similar chemical structure to vasopressin. Although lypressin is a non-endogenous family of vasopressin that is found naturally in pigs [51], demonstration of our biosensor's

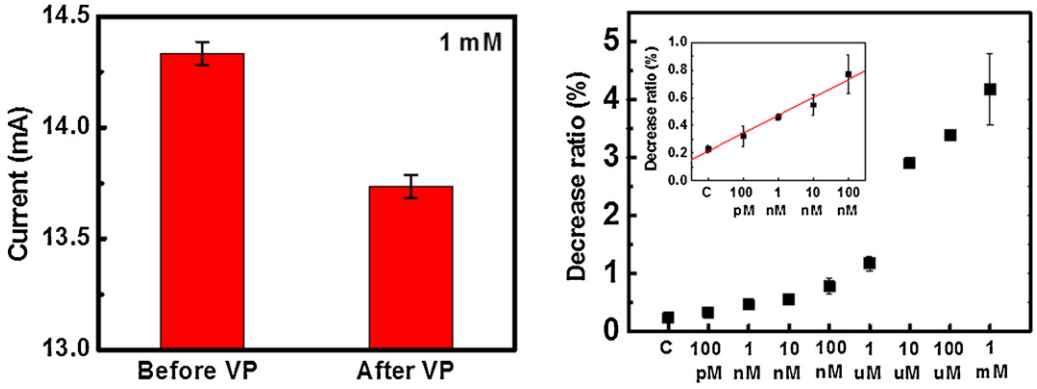

Fig. 3. Electrochemical detection of vasopressin standard solutions in aptamer-based microfluidic biosensors: (A) electrochemical signals measured before and after the introduction of vasopressin into the detection system and (B) calculated decrease ratios from measured electrochemical signals plotted against different vasopressin concentrations. The inset plot is the linear relationship between the signal decrease ratios and low vasopressin concentrations for limit-of-detection calculation. The error bars were calculated from three replicates.

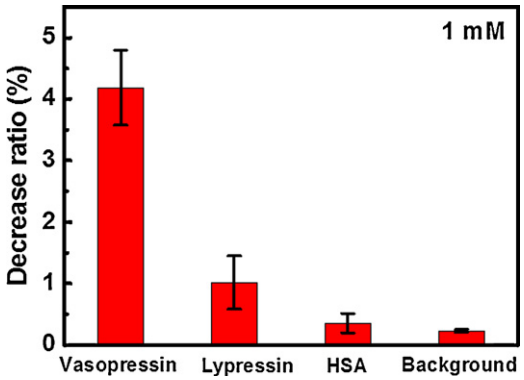

Fig. 4. Specificity measurement of vasopressin detection in aptamer-based microfluidic biosensors. The error bars were calculated from three replicates.

affinity for vasopressin over lypressin is strongly desired in order to demonstrate high sensor specificity. The specificity testing of the sensor was carried out in a standard solution that contained equal concentrations (1 mM) of HSA, arginine vasopressin and lypressin. As shown in Fig. 4, 1 mM vasopressin produced the largest current decrease ratio over background levels (about 4%). This is approximately 4-fold higher than that observed for lypressin and 12-fold higher than for HSA. Non-zero decrease ratios for the interferents could be the result of their non-specific binding to the aptamers. Furthermore, the higher decrease ratio for lypressin as compared to that of HAS could be attributed to lypressin's chemical resemblance to vasopressin that enables its partial conjugation to the aptamer. Although 1 mM vasopressin far exceeds plasma vasopressin concentration which is in the order of pM, HSA and lypressin have also been used at concentrations that exceed their known plasma levels. Lypressin, as mentioned, is a pig vasopressin that should not be present in human plasma, whereas the appropriate concentration for HSA is 0.6 mM [52]. Therefore, our preliminary results from the specificity test demonstrate the sensor's potential to monitor vasopressin in the presence of various interferents.

3.4. Continuous monitoring of vasopressin at different levels

Real-time electrochemical monitoring of target analytes in a point-of-care setting has recently been demonstrated for small-molecule drug cocaine [53], multidrug-resistant pathogens [54], and H1N1 influenza virus [55]. Here, we were able to demonstrate the ability of our biosensor to continuously monitor vasopressin concentrations in solution. The sensor's amperometric response was recorded by varying the vasopressin sample concentration. First, as shown in Fig. 5A the samples were introduced into the microfluidic system in order of increasing concentration. Then, as shown in Fig. 5B, the experiment was repeated with vasopressin samples introduced in order of decreasing concentration. Each solution was injected over the sensor for 10 s and the detection area was cleaned of vasopressin in between by injection of 0.01 M PBS solution for 10 s. The response of the sensor to changes in vasopressin concentration was found to be almost instantaneous. As expected, higher concentrations of vasopressin resulted in higher decrease in current. It can be inferred that the higher concentration of vasopressin injected over the aptamer-modified CNTs led to more vasopressin molecules binding at the immobilized aptamers. As discussed previously, this represents the loss of electron carriers on CNTs which was transduced to a decrease in current in our experiment. The binding affinity of the aptamer on the sensor's detection area should theoretically be constant under the same experimental conditions, which was demonstrated by the fact that current change due to the flow of a specified concentration of vasopressin was nearly the same for a given sensor.

3.5. Microfluidic biosensor performance in sheep serum samples

Serum is a very complex biological system that comprises among other things proteins, electrolytes, antibodies, antigens and hormones. As discussed previously, current vasopressin kits require complicated sample purification procedures in order to achieve the highest sensitivity possible. In order to demonstrate our sensor's potential to detect vasopressin within un-treated serum samples with sensitivity comparable to that of vasopressin assays, the sensors were tested in sheep serum. As shown in Fig. 6, vasopressin concentrations in serum ranging from 100 nM to 1 mM were detected, which confirms the capacity of the system to achieve detection at concentrations as low as 100 nM. The complicated serum composition imposes obstacle for the direct measurement of vasopressin without pretreatment. The electrolytes inside the serum act to neutralize the negative charge of the aptamer, which would partially impair the affinity of the aptamer loop structure. Further biosensor optimization and simple pretreatment of serum samples in the whole microfluidic system could significantly improve the detection sensitivity and specificity of the portable device for fast diagnosis.

3.6. Temperature effect on vasopressin detection

The reversible binding between aptamer and vasopressin is reportedly temperature dependent [26,27]. K_d, the dissociation constant of the aptamer–vasopressin complex is slightly higher

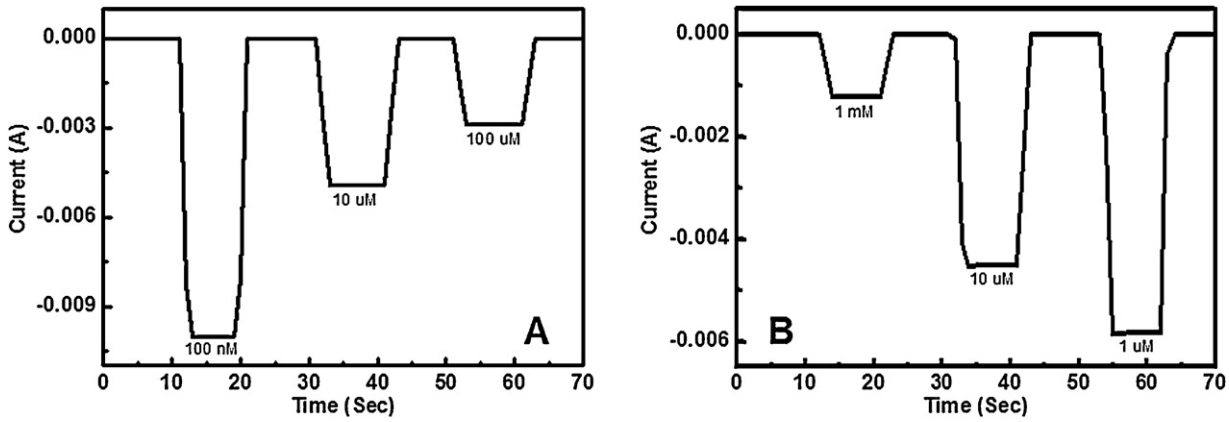

Fig. 5. Continuous monitoring of different vasopressin levels in aptamer-based microfluidic biosensors: (A) 100 nM, 10 μM, and 100 μM (increasing concentration trend) and (B) 1 mM, 10 μM, and 1 μM (decreasing concentration trend).

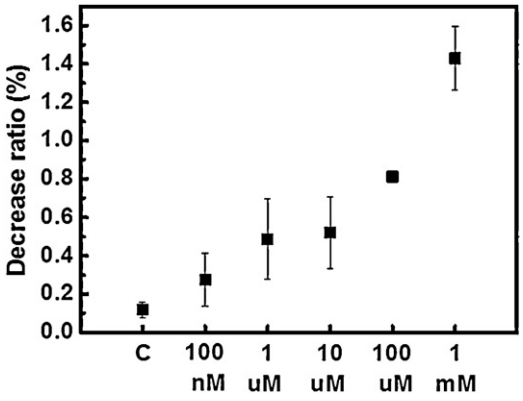

Fig. 6. Electrochemical detection of vasopressin-containing sheep serum in aptamer-based microfluidic biosensors. The error bars were calculated from three replicates.

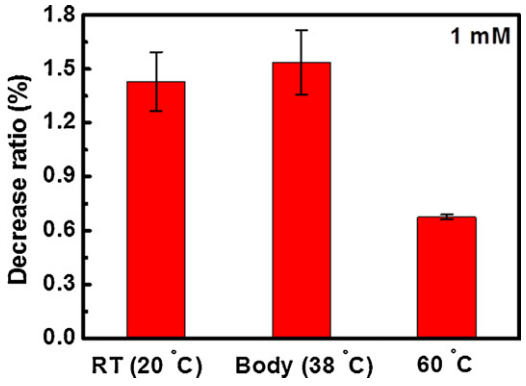

Fig. 7. Temperature effect on detection of vasopressin-containing sheep serum in aptamer-based microfluidic biosensors. The error bars were calculated from three replicates.

at room temperature as compared to body temperature, which strengthens the binding capability between aptamer and vasopressin and improves the detection performance as shown in Fig. 7. Increase in temperature can raise the measured K_d value, with the magnitude of the shift dependent on the thermodynamics of binding between DNA aptamers and molecular target system. Therefore, body temperature is optimal temperature for sensing because of increased van der Waals interactions and hydrogen bonding at the complex interface between vasopressin and aptamer. When the temperature approaches 60 °C, the disulfide bridge in vasopressin structure becomes chemically unstable which destroys the integrity of the vasopressin structure, resulting in the termination of vasopressin–aptamer binding. Thermally activated release of captured vasopressin reverses the biosensors back to the original state, which offers an opportunity for the repeated use of the device.

4. Conclusion

We demonstrated an electrochemical aptamer-based microfluidic biosensor for vasopressin detection with high sensitivity and specificity in standard solutions and sheep serum samples. The binding between vasopressin and aptamer depletes electron carriers on the CNT surface and reduce the local charge field resulting in a current decrease through the sensor. The miniaturization of device offers an opportunity to conduct biomarker detection from a trace amount of body fluids with high efficiency in a portable platform. The achieved limit-of-detection is 43 pM, which is of the same order as the physiological level of vasopressin in the bloodstream.

Acknowledgements

This work is financially supported by Office of Naval Research and was performed in part at the Cornell NanoScale Facility, a member of the National Nanotechnology Infrastructure Network, which is supported by the National Science Foundation (Grant ECS-0335765), and in part by the STC Program of the National Science Foundation under Agreement No. ECS-9876771. The authors thank Center for Nanoscale System at Cornell University and Professor Antje Baeumner in Department of Biological and Environmental Engineering at Cornell University for the use of electrochemical instruments.

References

[1] C. Sander, Science 287 (2000) 1977.
[2] J.H. Growdon, Arch. Neurol. 56 (1999) 281.
[3] D. Sidransky, Nat. Rev. Cancer 2 (2002) 210.
[4] P.S. Lu, Science 312 (2006) 337.
[5] Z. Gu, S.W. Belzer, C.S. Gibson, M.J. Bankowski, R.T. Hayden, J. Clinical Microbiology 41 (2003) 4636.
[6] N.V. Zaytseva, R.A. Montagna, A.J. Baeumner, Anal. Chem. 77 (2005) 7520.
[7] N. Wangoo, J. Kaushal, K.K. Bhasin, S.K. Mehta, C.R. Suri, Chem. Commun. (Cambridge, Engl.) 46 (2010) 5755.
[8] T.A. Addona, X. Shi, H. Keshishian, D.R. Mani, M. Burgess, M.A. Gillette, K.R. Clauser, D. Shen, G.D. Lewis, L.A. Farrell, M.A. Fifer, M.S. Sabatine, R.E. Gerszten, S.A. Carr, Nat. Biotechnol. 29 (2011) 635.
[9] E.D. Dawson, C.L. Moore, J.A. Smagala, D.M. Dankbar, M. Mehlmann, M.B. Townsend, C.B. Smith, N.J. Cox, R.D. Kuchta, K.L. Rowlen, Anal. Chem. 78 (2006) 7610.
[10] E. Suprun, T. Bulko, A. Lisitsa, O. Gnedenko, A. Ivanov, V. Shumyantseva, A. Archakov, Biosens. Bioelectron. 25 (2010) 1694.
[11] P.K. Sorger, Nat. Biotechnol. 26 (2008) 1345.
[12] P. Yager, T. Edwards, E. Fu, K. Helton, K. Nelson, M.R. Tam, B.H. Weigl, Nature 442 (2006) 412.
[13] J.D. Newman, A.P.F. Turner, Biosens. Bioelectron. 20 (2005) 2435.
[14] C. Liu, X. Qiu, S. Ongagna, D. Chen, Z. Chen, W.R. Abrams, D. Malamud, P.L.A.M. Corstjens, H.H. Bau, Lab Chip 9 (2009) 768.
[15] X. Xia, Y. Xu, X. Zhao, Q. Li, Anglais 55 (2009) 179.
[16] F. Najioullah, E. Combet, L. Paturel, J. Martial, L. Koulmann, L. Thomas, Y. Hatchuel, A. Cabié, R. Cesaire, Diagn. Microbiol. Infect. Dis. 69 (2011) 172.
[17] E. Stern, A. Vacic, N.K. Rajan, J.M. Criscione, J. Park, T.M. Fahmy, M.A. Reed, 10th IEEE International Conference on Solid-State and Integrated Circuit Technology (ICSICT), 2010, p. 1392.
[18] R.S. Gaster, D.A. Hall, C.H. Nielsen, S.J. Osterfeld, H. Yu, K.E. Mach, R.J. Wilson, B. Murmann, J.C. Liao, S.S. Gambhir, S.X. Wang, Nat. Med. 15 (2009) 1327.
[19] K.J. Hart, M.B. Wise, W.H. Griest, S.A. Lammert, Field Anal. Chem. Technol. 4 (2000) 93.
[20] H.B. Alam, E. Koustova, P. Rhee, World J. Surg. 29 (2005) S7.
[21] D. Morales, J. Madigan, S. Cullinane, J. Chen, M. Heath, M. Oz, J.A. Oliver, D.W. Landry, Circulation 100 (1999) 226.
[22] W.G. Voelckel, C. Raedler, V. Wenzel, K.H. Lindner, A.C. Krismer, C.A. Schmittinger, H. Herff, K. Rheinberger, A. Königsrainer, Crit. Care Med. 31 (2003) 1160.
[23] S. Song, L. Wang, J. Li, C. Fan, J. Zhao, TrAC Trends Anal. Chem. 27 (2008) 108.
[24] I. Willner, M. Zayats, Angew. Chem. Int. Ed. 46 (2007) 6408.
[25] T. Hianik, J. Wang, Electroanalysis 21 (2009) 1223.
[26] K.P. Williams, X.-H. Liu, T.N.M. Schumacher, H.Y. Lin, D.A. Ausiello, P.S. Kim, D.P. Bartel, Proc. Nat. Acad. Sci. USA 94 (1997) 11285.
[27] W.G. Purschke, D. Eulberg, K. Buchner, S. Vonhoff, S. Klussmann, Proc. Nat. Acad. Sci. USA 103 (2006) 5173.
[28] D. Eulberg, S. Klussmann, ChemBioChem 4 (2003) 979.
[29] Y.S. Huh, D. Erickson, Biosens. Bioelectron. 25 (2010) 1240.
[30] J. Zhu, T. Nguyen, R. Pei, M. Stojanovic, Q. Lin, Lab Chip 12 (2012) 3504.
[31] M. Li, J. Zhang, S. Suri, L.J. Sooter, D. Ma, N. Wu, Anal. Chem. 84 (2012) 2837.
[32] J. Zhang, P. Chen, X. Wu, J. Chen, L. Xu, G. Chen, F. Fu, Biosens. Bioelectron. 26 (2011) 2645.
[33] Y. Xiao, R.Y. Lai, K.W. Plaxco, Nat. Protocols 2 (2007) 2875.
[34] G. Herzog, D.W.M. Arrigan, Analyst 132 (2007) 615.
[35] O.A. Sadik, A.O. Aluoch, A. Zhou, Biosens. Bioelectron. 24 (2009) 2749.
[36] E.E. Ferapontova, E.M. Olsen, K.V. Gothelf, J. Am. Chem. Soc. 130 (2008) 4256.
[37] Y. Liu, N. Tuleouva, E. Ramanculov, A. Revzin, Anal. Chem. 82 (2010) 8131.
[38] Y. Lu, X. Li, L. Zhang, P. Yu, L. Su, L. Mao, Anal. Chem. 80 (2008) 1883.
[39] L. Bonel, J.C. Vidal, P. Duato, J.R. Castillo, Biosens. Bioelectron. 26 (2011) 3254.
[40] Y. Du, C. Chen, M. Zhou, S. Dong, E. Wang, Anal. Chem. 83 (2011) 1523.
[41] L. Barthelmebs, A. Hayat, A.W. Limiadi, J.-L. Marty, T. Noguer, Sens. Actuators B: Chem. 156 (2011) 932.
[42] J. Lee, M. Jo, T.H. Kim, J.-Y. Ahn, D.-k. Lee, S. Kim, S. Hong, Lab Chip 11 (2011) 52.
[43] K. Maehashi, K. Matsumoto, Sensors 9 (2009) 5368.
[44] P. Kara, A. de la Escosura-Muñiz, M. Maltez-da Costa, M. Guix, M. Ozsoz, A. Merkoçi, Biosens. Bioelectron. 26 (2010) 1715.

[45] H.-M. So, K. Won, Y.H. Kim, B.-K. Kim, B.H. Ryu, P.S. Na, H. Kim, J.-O. Lee, J. Am. Chem. Soc. 127 (2005) 11906.
[46] S. Jochberger, N.G. Morgenthaler, V.D. Mayr, G. Luckner, V. Wenzel, H. Ulmer, S. Schwarz, W.R. Hasibeder, B.E. Friesenecker, M.W. Dünser, J. Clin. Endocrinol. Metab. 91 (2006) 4381.
[47] R.W. Friddle, M.C. Lemieux, G. Cicero, A.B. Artyukhin, V.V. Tsukruk, J.C. Grossman, G. Galli, A. Noy, Nat. Nano 2 (2007) 692.
[48] E. Stern, J.F. Klemic, D.A. Routenberg, P.N. Wyrembak, D.B. Turner-Evans, A.D. Hamilton, D.A. LaVan, T.M. Fahmy, M.A. Reed, Nature 445 (2007) 519.
[49] G. Zheng, F. Patolsky, Y. Cui, W.U. Wang, C.M. Lieber, Nat. Biotechnol. 23 (2005) 1294.
[50] K. Maehashi, K. Matsumoto, Y. Takamura, E. Tamiya, Electroanalysis 21 (2009) 1285.
[51] A. Sharman, J. Low, Continuing Educ. Anaesth. Crit. Care Pain 8 (2008) 134.
[52] F. Yang, C. Bian, L. Zhu, G. Zhao, Z. Huang, M. Huang, J. Struct. Biol. 157 (2007) 348.
[53] J.S. Swensen, Y. Xiao, B.S. Ferguson, A.A. Lubin, R.Y. Lai, A.J. Heeger, K.W. Plaxco, H.T. Soh, J. Am. Chem. Soc. 131 (2009) 4262.
[54] J. Gottschamel, L. Richter, A. Mak, C. Jungreuthmayer, G. Birnbaumer, M. Milnera, H. Brückl, P. Ertl, Anal. Chem. 81 (2009) 8503.
[55] B.S. Ferguson, S.F. Buchsbaum, T.-T. Wu, K. Hsieh, Y. Xiao, R. Sun, H.T. Soh, J. Am. Chem. Soc. 133 (2011) 9129.